

Polarizable Solute in Polarizable and Flexible Solvents: Simulation Study of Electron Transfer Reaction Systems

Tateki Ishida[†]

Department of Computational Molecular Science, Institute for Molecular Science, Myodaiji, Okazaki 444-8585, Japan

Received: May 2, 2005; In Final Form: July 4, 2005

A polarizable solute model, based on the empirical valence bond approach, is developed and applied to electron transfer (ET) reactions in polarizable and flexible water solvents. The polarization effect is investigated in comparison with a nonpolarizable solute and solvent model. With free energy curves constructed by a molecular dynamics simulation, the activation energy barrier and the reorganization energy related to ET processes are investigated. The present simulation results show that the activation energy barrier becomes larger in the polarizable model than in the nonpolarizable model and that this makes the ET rate slower than that with the nonpolarizable model. It is shown that the effect of the electronic energy difference of solute molecule on free energy profiles is remarkable and that, corresponding to this effect, the reorganization energy is significantly modified. These results indicate that the process of solvent polarization by the polarized solute to enhance the solute–solvent interaction is a key factor and that treating the polarization of both solute and solvent at the same time is essential. Also, the polarization effect on the diffusive motion of the solute molecule in the polarization solvent is studied. The polarized solute molecule shows slower diffusive motion compared with that in the nonpolarizable model.

1. Introduction

The electron transfer (ET) reaction is one of the most important processes in chemical and biological systems. In particular, the ET mechanism in solution includes many significant physical aspects, and those have attracted many researchers. As seen in many studies to date, theoretical investigation of the ET process has developed an understanding of it along with a great deal of experimental data.^{1–3} For example, estimating rate constants for the ET reaction theoretically is one of the main purposes, and this is related to how to evaluate the activation energy and free energy difference of the ET reaction. Therefore, precise information on free energy curves in the ET process is required. The theory of the ET mechanism in solution due to Marcus^{3–5} has been well-recognized. Since it is based on the standard dielectric continuum theory, the microscopic representation of ET reactions is not enough. Also, it had been found that linear free energy relationship was one of the major concepts required to investigate these problems.^{6–8} Therefore, it has been attempted to describe free energy relationships at a microscopic level.^{9,10} Warshel¹¹ has proposed the corresponding energy gap treatment between reactant and product states to investigate ET reactions, and Warshel and co-workers^{11–14} have investigated the ET reaction process with the use of potential energy gap between reactant and product states as reaction coordinates, and they have pioneered simulation methods including the procedure for evaluating free energy relationships.

In the original theory by Marcus,^{4,5,15–18} it is assumed that free energy curves concerning ET reactions have a parabolic feature for both reactant and product states. In some ET reactions,^{19,20} the assumption of a parabolic free energy surface was found to be appropriate. However, many investigations of

charge separation reactions or ET reactions have indicated that assuming parabolic forms for the free energy curves of both reactant and product states is not suitable for analyses.^{14,21–23} Therefore, it has been considered that asymmetric features of free energy surfaces can be caused by nonlinear solute–solvent coupling effects. Until now, studies on the nonlinear solute–solvent coupling have been done with molecular dynamics simulations,^{14,24–26} and it has been investigated by a procedure based on integral equations.²⁷ Also, there have been theoretical and simulation studies including studies of quantum effects.^{19,28–33} Theoretically, how to derive the expression of free energy surfaces including the nonlinear effect has been an important issue for the study of ET reactions. Warshel¹¹ has given the expression for the curves and then some additional studies have been reported.^{14,34} In addition, important research on ET simulations with the polarizable water model has been reported by Warshel and co-workers.^{11,14} Ichiye²⁴ has discussed nonparabolic behavior on free energy surfaces using an ionic solvation model.²⁶ Also, Aqvist and Hansson³⁵ have investigated nonlinearity carefully. Recently, Matyushov and Voth³⁶ have developed a theory of ET, taking the asymmetric feature of the free energy surface and the solute and solvent polarizabilities into account, and they have developed a three-parameter model of ET in condensed phases with the linear relation between the two diabatic free energy surfaces holding. Also, they derived the nonparabolic free energy surfaces of ET reactions analytically, considering a two-state solute linearly coupled to a collective solvent mode with different force constants in the two solute electronic states.

In the study of solution phases, modeling solvation effects, in particular, how to have a model possess *physical reality*, is one of the most important factors. In simulation studies, many investigations have been devoted to improving the description of chemical processes in solutions.^{13,37–39} As one of the major

[†] E-mail: ishida@ims.ac.jp.

issues, incorporating explicit polarizability in solute and solvent molecules has been focused on. In particular, polarizable solvent water models have advanced the understanding of the insight of the electronic polarization in the solute–solvent interactions. Some of the treatments of polarizable solvent using the concept of induced dipole have been proposed by Warshel and co-workers,^{10,38,40} and the importance of treating solute polarization as responding to the solvent polarization has been shown by their works.¹⁰ Also, the importance of intramolecular flexibility in water models has been recognized for describing reactions in aqueous solution.^{41,42} There have been very few polarizable and flexible water models. Recently, Lefohn et al.⁴³ proposed a polarizable and flexible water model based on the empirical valence bond method,⁴⁰ and they showed a practical algorithm to include both polarizability and molecular flexibility into a water potential.

On the other hand, Morita and Kato⁴⁴ have applied the model based on the charge response kernel they proposed to the molecular dynamics simulation with the polarizable model both for solute and for solvent. Also, to the best of our knowledge, there have been few studies of a polarizable solute in a polarizable and flexible water solvent. The electrostatic field coming from polarizable solvent molecules can produce an electronic polarization effect on a solute molecule, and also, it is considered that the flexibility of solvent molecules enhances the fluctuation of the solvent field more. Then, the electronic polarization of the solute molecule is perturbed, and it will modify the curvature of the free energy surface. These effects are very important for the investigation of ET reactions in solution based on free energy surfaces. Therefore, if ET reactions are to be studied with a polarizable water model, the solute molecule itself also needs to be polarizable. To fulfill the above-mentioned requirements, in the current study, we adopt the two following features for a molecular dynamics study: (1) a solute molecule possesses two electronic states, which can be described by the EVB procedure;⁴⁰ (2) both solute and solvent are treated as polarizable.

In the case where the solute molecule is polarizable and has two electronic states, we can expect some features to be observed. First, since the solute electronic (internal) energy defined by the energy gap between two electronic states is taken into account, the important relation in the free energy difference between two representative states $\Delta G_P(X)$ and $\Delta G_R(X)$ (R denoted as a reactant state, P as a product state), which is due to Warshel,¹¹ is

$$\Delta G_P(X) - \Delta G_R(X) = X \quad (1)$$

where $X = V_P - V_R$, and V_P or V_R represents potentials in the P or R state of the ET, respectively. It is rewritten as the following

$$\Delta G'_P(X) - \Delta G_R(X) = X + \Delta E_{\text{int}} \quad (2)$$

where ΔE_{int} means the electronic energy difference between two states in the solute, and it should be noted that this term means the polarizability effect and that this is an obvious part of any polarizable model. It should be noted that $\Delta G'_P(X) = \Delta G_P + \Delta E_{\text{int}}$ and that the solvation energy, $\Delta G_{\text{sol}}^\circ$, is included in ΔG_P . Usually, in most works on ET reactions, this ΔE_{int} term is assumed to be 0, but when $\Delta E_{\text{int}} \neq 0$, the relative relation between minimum points for the reactant and product states will be changed, and corresponding to it, the point where two curves cross will be shifted. This indicates that the activation barrier height will be modified. These have been pointed out in the literature,²⁴ but there have been few studies using polarizable

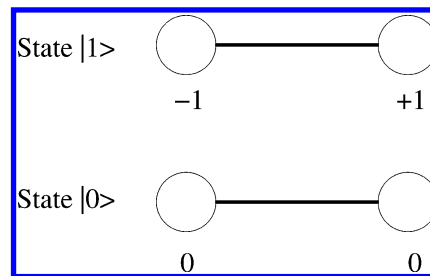


Figure 1. EVB states for the two-state ET system.

solute models. Second, in addition to the consideration of the role of solute electronic polarization in ET reactions based on free energy surfaces obtained, the molecular dynamics simulation enabled one to analyze dynamical properties of a polarizable solute molecule from its trajectory. To study these is of great interest in understanding the characteristics of polarizable solute models. In particular, as one of the properties, the self-diffusion of the solute molecule seems to be appropriate for studying. The effect of solute polarization on diffusive motion has been explored for the diffusion constants in the pyrazinyl radical and pyrazine systems whose components differ by only one hydrogen.⁴⁴ To focus on the solute polarization effect, it is considered that the polarizable solute model in the present study is suitable not only for investigating the effect of solute polarization on diffusive motion but also for checking the applicability of the model to studying dynamical properties of a polarizable solute model.

This paper is organized as follows. Section 2 briefly explains the polarizable solute molecule model employing the EVB treatment. Also, the procedure coupling with the so-called umbrella sampling is explained. The expression for the forces required for a molecular dynamics simulation is given in the Appendix. Section 3 describes simulation details in the present study. In section 4, the free energy surfaces obtained and the relation to ET reactions compared to nonpolarizable solute and solvent systems are discussed. Activation barrier height and reorganization energy in both polarizable and nonpolarizable models are compared, and the effect of polarization on ET rate is studied within the classical treatment. In addition, dynamical properties of the polarizable solute molecule in polarizable solvent are investigated. Conclusions are given in section 5.

2. Model Description

We consider the two-state solute model for a diatomic solute molecule in polarizable water in this paper. Here, we briefly explain the two-state solute model employing the EVB treatment by Warshel et al.⁴⁰ Also, for a polarizable and flexible water model, we employed the water model in ref 43; for details, it is recommended that readers refer to ref 43.

A. Two-State Solute Model. At first, the following two EVB diabatic basis states, corresponding to neutral and electron transferred states, $|0\rangle$ and $|1\rangle$, are set as seen in Figure 1. Then, the solute Hamiltonian is represented as follows:

$$H = H_{(\text{two-state system})} + V_{(\text{solute-solvent})} \quad (3)$$

$$H_{(\text{two-state system})} = |0\rangle h_0 \langle 0| + |1\rangle h_1 \langle 1| + |0\rangle h_{01} \langle 1| + |1\rangle h_{10} \langle 0| \quad (4)$$

$$V_{(\text{solute-solvent})} = |0\rangle V_0 \langle 0| + |1\rangle V_1 \langle 1| \quad (5)$$

Here h_0 and h_1 represent energies in EVB states in the gas phase, respectively. h_{01} and h_{10} mean the coupling terms between the

$|0\rangle$ and $|1\rangle$ states. Also, V_0 and V_1 indicate the solute–solvent interaction terms.

The ground, $|\phi_g\rangle$, and “excited”, $|\phi_e\rangle$, states are defined as

$$|\phi_g\rangle = c_0^{(g)}|0\rangle + c_1^{(g)}|1\rangle \quad (6)$$

$$|\phi_e\rangle = c_0^{(e)}|0\rangle + c_1^{(e)}|1\rangle \quad (7)$$

where $c_0^{(g)}$ and $c_1^{(g)}$ represent the coefficients for EVB basis state $|0\rangle$ and $|1\rangle$ in the ground-state wave function, respectively, and $c_0^{(e)}$ and $c_1^{(e)}$ those in the “excited” state.

On the basis of eqs 3–5 and 6, the ground-state solute Hamiltonian matrix with respect to the basis set $|0\rangle$ and $|1\rangle$ is described as

$$\begin{pmatrix} h_0 & h_{01} \\ h_{10} & h_1 \end{pmatrix} \quad (8)$$

where it should be noted that $h_0 < h_1$. In the present study, I treat the coupling terms, h_{10} and h_{01} , as constant, since estimating this term is not part of my present purpose. These are denoted as C , hereafter. Also, we set $h_0 = 0$, then the h_1 represents the energy difference, ϵ , between two diabatic states in a vacuum. Equation 8 is rewritten as

$$\begin{pmatrix} 0 & C \\ C & \epsilon \end{pmatrix} \quad (9)$$

where C means a constant value. In the MD simulation for aqueous solution, electrostatic field perturbation is added to the diagonal terms in a manner similar to the polarizable and flexible water simulation.⁴³ Therefore, we only need to set the electronic energy difference in a vacuum, i.e., ϵ . Then, solute–solvent interaction energy terms are added to diagonal elements in eq 9

$$\begin{pmatrix} V^{\text{state}(0)} & C \\ C & \epsilon + V^{\text{state}(1)} \end{pmatrix} \quad (10)$$

where $V^{\text{state}(0)}$ and $V^{\text{state}(1)}$ mean interaction terms for each state, respectively.

After diagonalizing eq 10, the coefficients, c_n ($n = 0$ or 1), for a linear combination representation of eq 6 in the ground state, are determined by eigenvectors obtained for two states. Using them, the effective partial charge on solute site i is estimated by

$$q_i = \sum_{n=0}^1 c_n^2 q_i^n \quad (11)$$

where q_i^n represents the charge on site i in EVB basis state $|n\rangle$ (see Figure 1).

B. Free Energy Surface Calculation. For generating free energy surfaces, it is required to sample the configuration space especially around the crossing point of the reactant and product diabatic curves. Therefore, an umbrella sampling method is employed in this study. In the usual case of a solute molecule with two states (reactant and product states), the Hamiltonian is represented so that two states are connected each other by interpolation, following the approach by Warshel and co-worker:¹⁴

$$H = T + (1 - \lambda)V_{\text{reactant}} + \lambda V_{\text{product}} \quad (12)$$

TABLE 1: Input Parameters for the Water Solvent Model⁴³

input parameter	
μ_z	1.85 D
α_{zz}	0.8074 Å ³
α_{yy}	0.8074 Å ³
α_{xx}	0.0000 Å ³

TABLE 2: Input Parameters for Oxygen (k_b Is the Boltzmann Constant)

$(\epsilon/k_b)/K$	$\sigma/\text{\AA}$
78.22	3.165

TABLE 3: Parameters for Solute Molecule (k_b Is the Boltzmann Constant)

mass/amu	$(\epsilon/k_b)/K$	$\sigma/\text{\AA}$
80	200	4.0

where T represents the kinetic energy term. V_{reactant} and V_{product} indicate potential energy terms for reactant and product states, respectively. λ is a parameter with $0 \leq \lambda \leq 1$.

Now, we extend the above-mentioned treatment to the two-state MS-EVB solute model. Modifying eq 3, the solute Hamiltonian is described as below

$$H = H_{(\text{two-state system})} + V'_{(\text{solute-solvent})} \quad (13)$$

$$V'_{(\text{solute-solvent})} = |0\rangle(1 - \lambda)V_0\langle 0| + |1\rangle\lambda V_1\langle 1| \quad (14)$$

where the term $H_{(\text{two-state system})}$ is the same as eq 4. The range of λ is $0 \leq \lambda \leq 1$.

Therefore, eq 10 is modified to the following equation:

$$\begin{pmatrix} (1 - \lambda)V^{\text{state}(0)} & C \\ C & \epsilon + \lambda V^{\text{state}(1)} \end{pmatrix} \quad (15)$$

3. Simulation Details

The system includes one diatomic solute and 252 water molecules. All simulations were performed with a time step of 0.5 fs and at 300 K. The system was set in a cubic cell with the periodic boundary condition, and a box length of 19.72 Å was used. A size of half of the box length was used for a cutoff. The simulations were carried out with the velocity leapfrog algorithm. The diatomic solute molecule was treated as a rigid body. The long-range Coulomb term was calculated using Ewald’s summation technique. The polarizable and flexible water makes use of an SPC/F⁴¹ classical water model, and all the parameters for the intramolecular potential energy are same as those used by Lefohn et al.⁴³ In the present study, the three-state model for water⁴³ is employed. Table 1 shows the dipole and polarizability employed as input for the water model. Also, the parameter of the oxygen site is given in Table 2.

For the solute molecule, the distance between two atomic sites is 2.5 Å, and the mass and the Lennard-Jones parameters are taken from the literature^{45,46} and are summarized in Table 3. The electronic energy difference, i.e., ϵ in eq 9, is set as 30 kcal/mol. For the electronic coupling term, i.e., C in eq 9, $C = 1$ kcal/mol is employed to represent weakly coupled adiabatic ET cases.^{47,48} At each time step, the average charges for each molecule are determined by employing the algorithm⁴³ for solvent. The calculation is carried out iteratively until the system energy converges within a criterion. In the present study, the criterion 1.0×10^{-7} au ($\approx 0.6 \times 10^{-4}$ kcal/mol) was used.

Two types of simulations were carried out. One was the simulation with the polarizable solute in the polarizable and flexible water model. The other was with the nonpolarizable

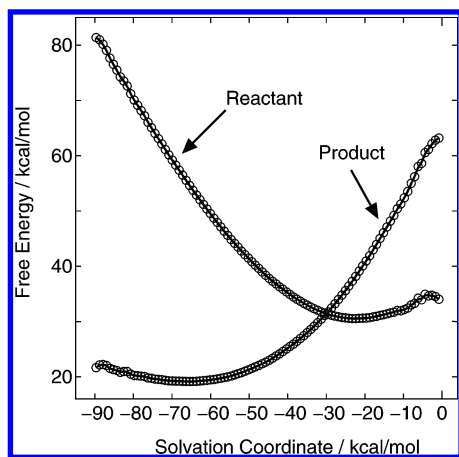


Figure 2. Free energy curves in the nonpolarizable model (see text). Note that the relation between reactant and product curves is $\Delta G_p^*(X) - \Delta G_R^*(X) = X + \Delta E_{\text{int}}$ (eq 2).

solute in nonpolarizable water model for comparison, and the SPC water model for nonpolarizable water was employed. Hereafter, the former model is denoted as a polarizable model (polarizable both for solute and for solvent) and the latter as a nonpolarizable model (nonpolarizable both for solute and for solvent).

At first, the simulation with only 256 polarizable and flexible water molecules was carried out for 500 ps to achieve equilibration. After that, water molecules within the sphere which can embrace a solute molecule at the center of the simulation box were removed, and then, the diatomic solute molecule was set there. In all simulations, equilibration runs were performed for 100 ps before the 150 ps production run. The system temperature was controlled by using the velocity rescaling. The system temperature was allowed to vary ± 5 K around 300 K.

To construct free energy profiles, a series of 11 window samplings were performed with λ in eqs 21–24 selected equal to 0.0, 0.1, 0.2, 0.3, 0.4, 0.5, 0.6, 0.7, 0.8, 0.9, and 1.0. The simulation results were combined using the weighted histogram analysis method.^{49,50} The solvation energy was estimated based on the results at different λ values.¹⁴ Refer to refs 14, 49, and 50 for details. Also, to estimate the mean square displacement of the solute molecule, data collection was done every 1 fs during the production run.

4. Results and Discussion

A. Free Energy Surface Profiles. Figure 2 shows free energy curves with nonpolarizable models both for solute and for solvent. In Figure 3, free energy curves for the system consisting of the polarizable solute in polarizable solvent are displayed. The free energy difference between two minimum points (the minimum point of product relative to reactant) is -13.6 kcal/mol for the nonpolarizable model and -0.9 kcal/mol for the polarizable model, respectively. On the other hand, the solvation energy, ΔG_{sol}^0 , is -43.6 kcal/mol in Figure 2 and -30.9 kcal/mol in Figure 3, respectively. Therefore, these results mean that the electronic energy difference between two states in the solute, ΔE_{int} (ϵ in eq 10), is strongly affected by the relative position between two free energy curves. The solute dipole moment in the nonpolarizable system is 12.01 D, and in the polarizable system, it is estimated to be 11.99 D as a averaged value from the simulation results. Compared with the solvation energy in the nonpolarizable system, the value of it in the polarizable system is reduced by about 13 kcal/mol, even though the difference of the solute dipole between in the nonpolarizable

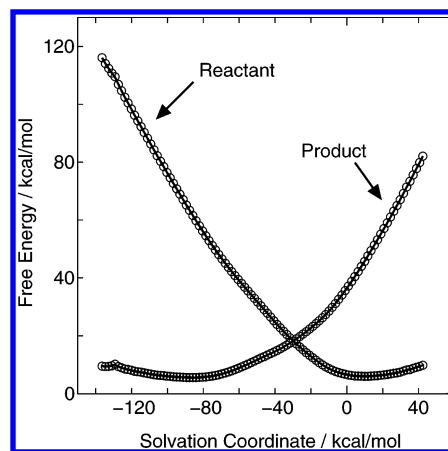


Figure 3. Free energy curves in the polarizable model (see text). Note that the relation between reactant and product curves is $\Delta G_p^*(X) - \Delta G_R^*(X) = X + \Delta E_{\text{int}}$ (eq 2).

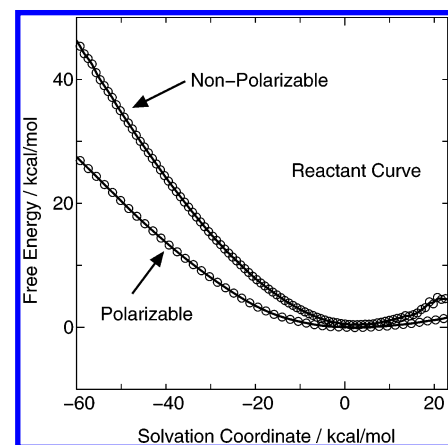


Figure 4. Comparison of free energy curves of reactant between in the nonpolarizable and in the polarizable model. Note that two curves are displayed coinciding at the minimum point for comparison.

and the polarizable systems is not large (0.02 D). This result indicates that the solvation of the polarizable solute is less enhanced by the polarization effect of the solvent molecules in the system. In the solvation process of polarized solute, the solute polarizes the solvent to enhance the solute–solvent interaction energy, and then, the work in polarizing solvent decreases the free energy. On the basis of this, the energy that the polarized solute cost to polarize solvent in the polarizable solvent is obviously considered to be larger compared with that in the nonpolarizable solvent. Therefore, the difference of the solvation energy between that in the polarizable model and that in the nonpolarizable model is consistent with the above-mentioned discussion of the solvation of polarized solute.

Also, the comparison of free energy curves between that in the nonpolarizable model and that in the polarizable model is shown for the reactant curve in Figure 4 and the product curve in Figure 5, respectively. As seen in Figures 4 and 5, the curvature of the polarizable model in both the reactant state and the product state becomes smaller than those of the nonpolarizable model. Considering ΔE , which is the difference of the potential energy in each diabatic state, and $\delta\Delta E = \Delta E - \langle\Delta E\rangle$, it is expected that the smaller the ΔE is, the larger the curvature becomes. On the basis of results in the present study, the polarization effect on solute molecule indicates that it makes the energy state of the product higher compared with that in the nonpolarizable solute model, and it is considered that the fluctuation of the energy difference between two diabatic states in the polarizable model is enhanced more than that in the

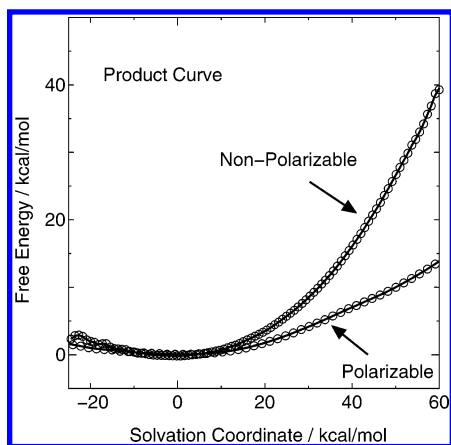


Figure 5. Comparison of free energy curves of product between in the nonpolarizable and in the polarizable model. Note that two curves are displayed coinciding at the minimum point for comparison.

TABLE 4: Activation Barrier, ΔG^\ddagger , and Reorganization Energy, λ

	ΔG^\ddagger /(kcal/mol)	λ (product state)/(kcal/mol)
nonpolarizable solute	0.61	19.85
polarizable solute	12.12	40.08

nonpolarizable model. In addition, in the polarizable model, the polarization effect on solvent caused by the polarized solute makes the solute energy higher for the compensating energy cost needed to polarize the solvent. Therefore, $\delta\Delta E$ has a larger variation in the polarizable model, and the curvature of free energy surfaces is expected to be smaller than that in the nonpolarizable model. This expectation is consistent with the present simulation result. Also, considering these results from the point of view related to the dielectric saturation²¹ seems to be important. If the dielectric saturation effect would be dominant, solvent molecules tended to align in the solute electric field. Then, the fluctuation, $\delta\Delta E$, would be reduced and the curvature of free energy surfaces would be large. However, our simulation results show an opposite tendency. This implies that the dielectric saturation effect is less dominant in our polarizable solute and solvent model. Therefore, in our model, it is considered that the solvent molecules which are around a solute molecule tend to be “free” to a certain extent (partly due to the possibility of the effect of the solvent flexibility) rather than to coordinate to the solute in any order.

B. Activation Barrier and Reorganization Energy. In Table 4, the activation barrier and reorganization energy estimated from free energy surfaces are summarized. In the nonpolarizable model, the activation barrier is very small (0.61 kcal/mol). In contrast, it becomes larger (12.12 kcal/mol) in the polarizable model, even though the curvature of free energy curves with the polarizable solute and solvent is smaller than that with the nonpolarizable solute and solvent. Here, it should be noted that the electronic energy difference between two states in the solute, ΔE_{int} , is taken into account in the free energy surfaces in Figures 2 and 3. Therefore, as discussed previously, the effect of ΔE_{int} is very important not only for the relation between the two curves but also for the activation barrier height. These features have been discussed in a charge separation reaction, $D^0 + A^0 \rightarrow D^+ + A^-$ (D, donor; A, acceptor), in a MeCl-like solvent, assuming that the solute–solvent interactions are unchanged by the variation of ΔE_{int} .²⁴ As shown by Warshel,¹¹ ΔG^\ddagger is estimated by the intersection of free energy curves. In the present study, electronic energy difference is effective. Therefore, it is expected that the larger ΔE_{int} is, the larger ΔG^\ddagger becomes. Figures 2 and 3 indicate that the free energy difference between that at

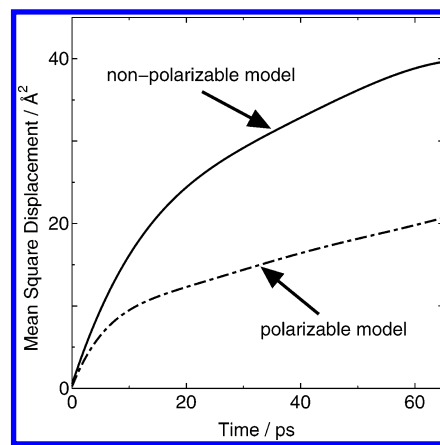


Figure 6. Mean square displacement of the center of mass of solute.

the minimum point and that at the *solvation coordinate* = $-\Delta E_{\text{int}}$ (this point corresponds to the crossing point between two curves in Figures 2 and 3), i.e., ΔG^\ddagger , becomes smaller in the nonpolarizable model than in the polarizable model. Therefore, our simulation results are consistent with the expectation deduced from the same method as Warshel demonstrated.¹¹ The present study shows that the correlation between the polarizable effect and the electronic energy difference of solute molecule makes the ET rate slower in comparison with that in the nonpolarizable solute and solvent system.

Corresponding to the shift of the crossing point between two curves, Table 4 shows that the reorganization energy in the polarizable model becomes larger than in the nonpolarizable model. This corresponds to the situation that the configuration of solvent in the reactant state is not appropriate for the product state and needs to be adjusted. Then, since the solute molecule is polarized by transferring from the reactant to the product, solvent molecules also need to be polarized in the polarizable model. As mentioned before, the physical interpretation of this polarization effect means raising the solute energy of product state, and therefore, it is considered that the degree of the positive increase of the free energy in the product state becomes larger than that in the nonpolarizable model.

C. Characteristic Dynamical Property in the Polarizable Solute and Solvent System. In addition to free energy profiles, we discuss a dynamical property of the polarized model we employed. In Figure 6, the mean square displacement of the solute molecule in the product state both in the nonpolarizable model and in the polarizable model is displayed. The difference of diffusive motion between the two models is remarkable, and it is found that the diffusive motion in the polarizable model becomes slower than that in the nonpolarizable model. This feature is consistent with the results of pyrazine and pyrazinyl radical system including the polarizable effect.⁴⁴ The estimated average solute–solvent interaction energy, E_{uv} , from simulation data is -42.3 kcal/mol in the nonpolarizable model and -47.0 kcal/mol in the polarizable model, respectively. These are acceptable results in good accord with the polarization effect on both solute and solvent in the polarizable model. In addition, these explicitly mean that the binding energy between solute and solvent is larger in the polarizable model compared with that in the nonpolarizable model, and the strong binding causes the slow diffusive motion of the solute in the polarizable model.

In summary, our result indicates that, even without any difference in the solute molecule structure and size, the polarization of solute and solvent is effective due to the diffusive motion. This is one of the primary results in the present study. Also, including the polarization effect is considered to be

essential for a detailed investigation of dynamical properties. Therefore, the polarizable model we used in the current study is suitable not only for the estimation of the free energy curve but also for studying dynamical properties.

5. Conclusion

The polarizable model for solute based on the EVB approach was employed in the present study with a polarizable and flexible water model. It was applied to ET reaction problems. To construct free energy profiles, a molecular dynamics simulation was performed combined with window sampling.

From free energy curve profiles, the free energy difference between two curves in the polarizable model became smaller compared with that in the nonpolarizable model, even though the difference in solute dipole was not large (0.02 D). The result indicates that the solvation of the polarizable solute in the polarizable solvent is less enhanced. This result indicates that the electronic energy difference between two states in the solute, ΔE_{int} , has a large effect on the relative position between two free energy curves. In addition, this is due to the polarization effect on solvent caused by the polarized solute, which increases the solute–solvent interaction, but in compensation for that, costs the energy needed to polarize the solvent. This effect appears clearly in the polarizable model which is different from that in the nonpolarizable model.

The comparison of free energy curvatures between the nonpolarizable and the polarizable model was done. In both the reactant and the product states, curvatures in the polarizable model were smaller than those in the nonpolarizable model. This implies that the fluctuation of the energy difference between two diabatic states is more enhanced in the polarizable model. In addition, considering that the polarization effect on the solvent by the polarized solute makes the solute energy of the product state higher than that in the nonpolarizable model, these results are understandable. Also, the present result was discussed relative to the dielectric saturation. In the present study, our simulation results indicate that the dielectric saturation effect is not so dominant. Therefore, in our simulation results show that, under the situation with the polarizable solute and solvent, solvent molecules around a solute molecule are likely to be “free” to a certain extent (partly due to the possibility of the effect of solvent flexibility) instead of coordinating to the solute in any order, as in the case where the dielectric saturation is remarkably effective.

The analysis of the activation barrier and reorganization energy was carried out based on the free energy curves obtained. In the nonpolarizable model, the activation barrier was estimated to be 0.61 kcal/mol. It was 12.12 kcal/mol in the polarizable model. It was found that the electronic energy difference of the solute was an important factor for determining the barrier height in ET reaction processes. These show that, with the polarizable solute and solvent model, the polarization effect and the electronic energy difference of solute decreases the ET rate in comparison with that with the nonpolarizable solute and solvent model. Also, corresponding to the crossing point shifting, the reorganization energy in the polarizable model was larger than that in the nonpolarizable model. It was found that this is related to the increased solute energy of the product state due to the polarization of the solvent by the polarized solute.

In addition to the free energy profiles for ET reactions, an investigation of dynamical properties of the polarizable solute in polarizable solvent was performed. As one of the dynamical properties, the diffusive motion of the solute molecule was observed. It is found that the diffusive motion in the polarizable

model is clearly slower than that in the nonpolarizable model and that the estimation of solute–solvent interaction energy shows that the binding energy is stronger in the polarizable model. Our result indicates that the polarization of solute and solvent is very important to the diffusive motion even though there is no difference in the solute molecule structure and size. Therefore, the polarization effect is essential for the study of dynamical properties. The polarizable solute and solvent model used in the present study seems to be useful for the detailed study of the solution system.

Acknowledgment. The author gratefully thanks Professor Gregory A. Voth for valuable comments and for his guiding the author to this work. Also, the author is grateful to Professor A. Morita for helpful comments.

Appendix: Force Expression for MD Simulation

Forces on the solute molecule in two diabatic states are calculated in the field coming from solvent effective charges. Therefore, the forces acting on site i of the solvent or solute molecules are described below.

(a) For Solvent Molecule. Noting that $q_j^{\text{state}(n)}$ means the solute site j in the diabatic state n , the force representations in the real-space are the following:

$$F_{r1}^{(v)} = - \sum_{j \in \text{solute}} q_i \left\{ \nabla_i \left(\frac{\text{erfc}(\alpha r_{ij})}{r_{ij}} \right) \right\} q_j^{\text{state}(n)} \quad (16)$$

where erfc is the complementary function.

Also, forces in the Fourier space are described as

$$F_{k1}^{(v)} = - \frac{4\pi}{V} \sum_{k \neq 0} A_k \mathbf{k}_\alpha \text{Im} [q_i e^{-i\mathbf{k}\cdot\mathbf{r}_i} \sum_{j=1}^{N_s} q_j e^{i\mathbf{k}\cdot\mathbf{r}_j}] \quad (17)$$

where Im indicates the imaginary part and the real part is in brackets, respectively. Here, $A_k = \exp(-k^2/4\alpha^2)/k^2$, and $\mathbf{k}_\alpha = \{k_x, k_y, k_z\}$.

(b) For Solute Molecule. As previously mentioned, the solute molecule has two sites in our model, which coincide with atomic sites of the solute. Also, it was assumed that the two atomic sites possess only charges. Therefore, forces acting on the sites which possess charges in the real and Fourier spaces are denoted by $F_{r_c}^{(u)}$ and $F_{k_c}^{(u)}$:

$$F_{r_c}^{(u)} = - \sum_{j \in \text{solvent}} q_i^{\text{state}(n)} \left\{ \nabla_i \left(\frac{\text{erfc}(\alpha r_{ij})}{r_{ij}} \right) \right\} q_j \quad (18)$$

$$F_{k_c}^{(u)} = - \frac{4\pi}{V} \sum_{k \neq 0} A_k \mathbf{k}_\alpha \text{Im} [q_i^{\text{state}(n)} e^{-i\mathbf{k}\cdot\mathbf{r}_i} \sum_j q_j e^{i\mathbf{k}\cdot\mathbf{r}_j}] \quad (19)$$

where Im , A_k , and \mathbf{k}_α are the same as in the solvent case.

References and Notes

- (1) Kuznetsov, A. M., Ulstrup, J., Eds. *Electron Transfer in Chemistry and Biology: An Introduction to the Theory*; Wiley: Chichester, U.K., and New York, 1999.
- (2) Kuznetsov, A. M., Ed.; *Charge Transfer in Physics, Chemistry and Biology: Physical Mechanisms of Elementary Processes and an Introduction to the Theory*; Gordon and Breach Science Publishers: Luxembourg, 1995.
- (3) Marcus, R. A.; Sutin, N. *Biochim. Biophys. Acta* **1985**, *811*, 265.
- (4) Marcus, R. A. *Discuss. Faraday Soc.* **1960**, *29*, 21.
- (5) Marcus, R. A. *J. Chem. Phys.* **1965**, *43*, 679.
- (6) Marcus, R. A. *J. Phys. Chem.* **1968**, *72*, 891.
- (7) Marcus, R. A. *Annu. Rev. Phys. Chem.* **1964**, *15*, 155.

- (8) Hush, N. S. *J. Chem. Phys.* **1958**, 28, 296.
(9) Warshel, A. *Proc. Natl. Acad. Sci. U.S.A.* **1984**, 81, 444.
(10) Hwang, J. K.; King, G.; Creighton, S.; Warshel, A. *J. Am. Chem. Soc.* **1988**, 110, 5297.
(11) Warshel, A. *J. Phys. Chem.* **1982**, 86, 2218.
(12) Churg, A. K.; Weiss, R. M.; Warshel, A.; Takano, T. *J. Phys. Chem.* **1983**, 87, 1683.
(13) Hwang, J.-K.; Warshel, A. *J. Am. Chem. Soc.* **1987**, 109, 715.
(14) King, G.; Warshel, A. *J. Chem. Phys.* **1990**, 93, 8682.
(15) Marcus, R. A. *J. Chem. Phys.* **1956**, 24, 966.
(16) Marcus, R. A. *J. Chem. Phys.* **1956**, 24, 979.
(17) Marcus, R. A. *J. Chem. Phys.* **1957**, 26, 867.
(18) Marcus, R. A. *J. Chem. Phys.* **1957**, 26, 872.
(19) Warshel, A.; Hwang, J.-K. *J. Chem. Phys.* **1986**, 84, 4938.
(20) Kuharski, R. A.; Bader, J. S.; Chandler, D.; Sprik, M.; Klein, M.; Impey, R. W. *J. Chem. Phys.* **1988**, 89, 3248.
(21) Hatano, Y.; Saito, M.; Kakitani, T.; Mataga, N. *J. Phys. Chem.* **1988**, 92, 1008.
(22) Carter, E. A.; Hynes, J. T. *J. Phys. Chem.* **1989**, 93, 2184.
(23) Yoshimori, A.; Kakitani, T.; Enomoto, Y.; Mataga, N. *J. Phys. Chem.* **1989**, 93, 8316.
(24) Ichiye, T. *J. Chem. Phys.* **1996**, 104, 7561.
(25) Bader, J. S.; Berne, B. J. *J. Chem. Phys.* **1996**, 104, 1293.
(26) Yelle, R. B.; Ichiye, T. *J. Phys. Chem. B* **1997**, 101, 4127.
(27) Chong, S.-H.; Hirata, F. *J. Chem. Phys.* **1997**, 106, 5225.
(28) Fischer, S. F. *J. Chem. Phys.* **1970**, 53, 3195.
(29) van Duyne, R. P.; Fischer, S. F. *Chem. Phys.* **1974**, 5, 183.
(30) Wolynes, P. G. *J. Chem. Phys.* **1987**, 87, 6559.
(31) Warshel, A.; Chu, Z. T.; Parson, W. W. *Science* **1989**, 246, 112.
(32) Cao, J.; Voth, G. A. *J. Chem. Phys.* **1997**, 106, 1769.
(33) Ungar, L. W.; Newton, M. D.; Voth, G. A. *J. Phys. Chem. B* **1999**, 103, 7367.
(34) Zhou, H.-X.; Szabo, A. *J. Chem. Phys.* **1995**, 103, 3481.
(35) Aqvist, J.; Hansson, T. *J. Phys. Chem.* **1996**, 100, 9512.
(36) Matyushov, D. V.; Voth, G. A. *J. Chem. Phys.* **2000**, 113, 5413.
(37) Warshel, A. *Chem. Phys. Lett.* **1978**, 55, 454.
(38) Warshel, A. *J. Phys. Chem.* **1979**, 83, 1640.
(39) Warshel, A.; Russell, S. T. *Q. Rev. Biophys.* **1984**, 17, 283.
(40) Warshel, A.; Weiss, R. M. *J. Am. Chem. Soc.* **1980**, 102, 6218.
(41) Toukan, K.; Rahman, A. *Phys. Rev. B* **1985**, 31, 2643.
(42) Dang, L. X.; Pettitt, B. M. *J. Chem. Phys.* **1987**, 91, 3349.
(43) Lefohn, A. E.; Ovchinnikov, M.; Voth, G. A. *J. Phys. Chem. B* **2001**, 105, 6628.
(44) Morita, A.; Kato, S. *J. Chem. Phys.* **1998**, 108, 6809.
(45) Bursulaya, B. D.; Zichi, D. A.; Kim, H. J. *J. Phys. Chem.* **1995**, 99, 10069.
(46) Bursulaya, B. D.; Zichi, D. A.; Kim, H. J. *J. Phys. Chem.* **1996**, 100, 1392.
(47) Newton, M. D. *Chem. Rev.* **1991**, 91, 767.
(48) Creutz, C. *Prog. Inorg. Chem.* **1983**, 30, 1.
(49) Ferrenberg, A. M.; Swendsen, R. H. *Phys. Rev. Lett.* **1989**, 63, 1195.
(50) Kumar, S.; Bouzida, D.; Swendsen, R. H.; Kollman, P. A.; Rosenberg, J. M. *J. Comput. Chem.* **1992**, 13, 1011.